Journal of Zhejiang University-SCIENCE A (Applied Physics & Engineering)
ISSN 1673-565X (Print); ISSN 1862-1775 (Online)
www.zju.edu.cn/jzus; www.springerlink.com
E-mail: jzus@zju.edu.cn

A rotary ultrasonic motor using radial bending mode of ring with nested PZT excitation*

Ying-xiang LIU†, Jun-kao LIU, Wei-shan CHEN, Xiao-hui YANG

(*State Key Laboratory of Robotics and System, Harbin Institute of Technology, Harbin 150001, China*)

†E-mail: liuyingxiang868@163.com

Received Aug. 19, 2011; Revision accepted Oct. 24, 2011; Crosschecked Feb. 7, 2012

Abstract: This study presents and verifies a new idea for constructing a rotary traveling wave ultrasonic motor (USM) that uses the radial bending mode of a ring. In the new design, 20 trapezoid cross section slots are cut symmetrically in the outer surface of a thick duralumin alloy ring, where 20 PZT stacks are nested. In each slot, two wedging blocks are set between the PZT stack and the two sides of the slot respectively to apply preloading on the PZT ceramics. Two radial bending modes of the stator that have a phase difference of a quarter wavelength on space are generated by using the d_{33} operating mode of the PZT elements, and then a flexural traveling wave is formed by the superimposing of two standing waves whose amplitudes are equal and phases are different by 90° temporally. Two conical rotors are pressed to each end of the ring type stator by a coiled spring. The finite element method (FEM) simulation is developed to validate the feasibility of the proposed motor. The maximal speed and torque of the prototype are tested to be 126 r/min and 0.8 N·m, respectively.

Key words: Rotary ultrasonic motor, Radial bending mode, Traveling wave, Wedging block clamped structure
doi:10.1631/jzus.A1100225 **Document code:** A **CLC number:** TM356

1 Introduction

Ultrasonic motors (USMs) exhibit properties such as low speed, large output force, high power density, high position accuracy, simple structure, self-locking when the power is off and nonelectromagnetic radiation (Ueha and Tomikawa, 1993; Zhao, 2010). These advantages ensure that they are good candidates for aerospace mechanism, semiconductor manufacturing system, precision machine tool, high precision positioning platform and micro electromechanical system (MEMS). According to the operating modes of the PZT elements, USM may be classified into bonded type motor (Park *et al*., 2005; Ting *et al*., 2007; Luo *et al*., 2008; Sun *et al*., 2010) and sandwiched type motor (Asumi *et al*., 2009; Chen *et al*., 2010; Liu *et al*., 2010a; Shi *et al*., 2010). For a bonded type motor, the stator is usually constructed by gluing the PZT ceramic to an elastic metal body with conductive adhesive, and the ultrasonic vibration of the stator is excited by the d_{31} operating mode of the PZT element.

Amongst various bonded type motors, the classic ring type traveling wave USM (Li *et al*., 2007; Zhang and Tan, 2008; Oh *et al*., 2009) maybe the most successful member with its advantages of clear working principle and simple fabrication. It has also been commercially used in a camera auto-focus system. However, as it is finding applications in other fields, such as in robot joint driving and actuation of space mechanism, its output ability is found to be relatively insufficient. Firstly, the d_{31} mode of the PZT used by this motor has a lower electromechanical coupling factor. Secondly, this motor exhibits the demerits of the adhesive layer and PZT fatigues under intensive vibration. Furthermore, to the axial bending mode of the elastic ring, the vibration amplitudes of

* Project supported by the National Natural Science Foundation of China (Nos. 50875057 and 51105097), and the State Key Laboratory of Robotics and Systems (No. SKLRS200901A04), China

teeth surface points have obvious differences in both axial and circumferential directions. All these factors make it difficult to obtain high torque and efficiency.

To avoid the previous drawbacks in the classic ring type traveling wave USM, the traveling wave motor excited by the sandwich transducer is a good choice. Iula *et al.* (2010) used four high power Langevin transducers to excite the traveling wave in a cylindrical stator, and their prototype exhibited a static torque of about 0.94 N·m. Petit and Gonnard (2009) proposed a double ring type traveling wave USM excited by four longitudinal actuators, and their prototype achieved a torque of 0.08 N·m. Jin and Zhao (2008) investigated a rotary USM using a composite transducer, and the maximal torque of the prototype was 0.25 N·m. Liu *et al*. (2010b) studied a traveling wave motor in which four Langevin transducers were coupled to a cylindrical stator through exponential shape horns, and the prototype achieved a maximal torque of 1.95 N·m. Liu *et al*. (2010c) also proposed an improved cylindrical traveling wave USM using only one longitudinal and bending composite transducer. All these initiatives soundly prove that most of the USM using the d_{33} operating mode of PZT have potentiality to obtain higher output torque and power. However, one common disadvantage amongst these designs is that the vibration coupling interface from the actuating sandwich transducer to the stator usually leads to a deformed traveling wave, and thus vibration energy is greatly consumed at the interface. Furthermore, for these motors, it is a common feature that the longitudinal or bending mode of a transducer is utilized to generate a standing wave in the ring type or cylindrical stator, which requires a good match between the vibration modes of the transducer and the stator. In fact, it is a difficult design work to touch and bring constraint to the structure.

This study proposes a new ring type stator structure for a traveling wave USM, which is composed of a duralumin alloy ring with PZT stacks nested in the trapezoid slots of the ring's outer surface and wedging blocks set between the PZT stack and the two sides of the slot to apply preloading on the PZT ceramics. In this new design, the radial bending mode of the ring type stator, which can result in nearly identical vibration trajectories on the driving particles, is generated by using the d_{33} operating mode of the PZT. The PZT elements work with compression stress state and no tensile failure will occur under intensive vibration, and thus strong excitation can be applied to achieve higher output. Furthermore, as two radial bending modes with the same order are used to generate a traveling wave in the stator, modal degeneration can be easily realized by the symmetrical structure. No vibration coupling problem between the transducer and stator exists in this new design, which is very significant to improve the quality of the traveling wave. Thus, the proposed motor not only inherits the advantages of both the classic ring type traveling wave USM and the motor excited by sandwich transducer, but also overcomes their disadvantages. The structure and the fabrication of the proposed motor are introduced. A prototype is designed and analyzed using the finite element method (FEM). Finally, the vibration and mechanical output characteristics of the prototype are tested.

2 Structure and working principle of the USM

Fig. 1 shows the structure of the proposed motor, which is composed of subassemblies of stator and rotor. In the stator subassembly, 20 trapezoid cross section slots are cut symmetrically on the outer surface of a thick ring, where 20 PZT stacks are nested. Sixty driving teeth are cut uniformly on the inner surface of the ring. Each PZT stack contains two pieces of PZT ceramics, and a thin beryllium bronze sheet is clamped between the two PZT ceramics to act as an electrode. In each slot, two wedging blocks are set between the PZT stack and the two sides of the slot to apply preloading on the PZT ceramics. Thin rubber sheets are set between the PZT stacks and the bottoms of the slots to serve as insulating layers. The structure of the rotor subassembly is shown in Fig. 1b. Two conical rotors are pressed to each end of the ring type stator by a coiled spring. Note that the polarization directions and excitations of the PZT stacks should be assigned as shown in Fig. 1c, and the metal ring serves as the common electrode for all PZT ceramics. All the PZT elements are polarized along their thickness directions, and the d_{33} operating mode is used to excite the radial bending modes of the stator.

In the fabrication of the stator, the sum thickness dimension of one PZT stack and two wedging blocks is made slightly larger than the width of the nesting

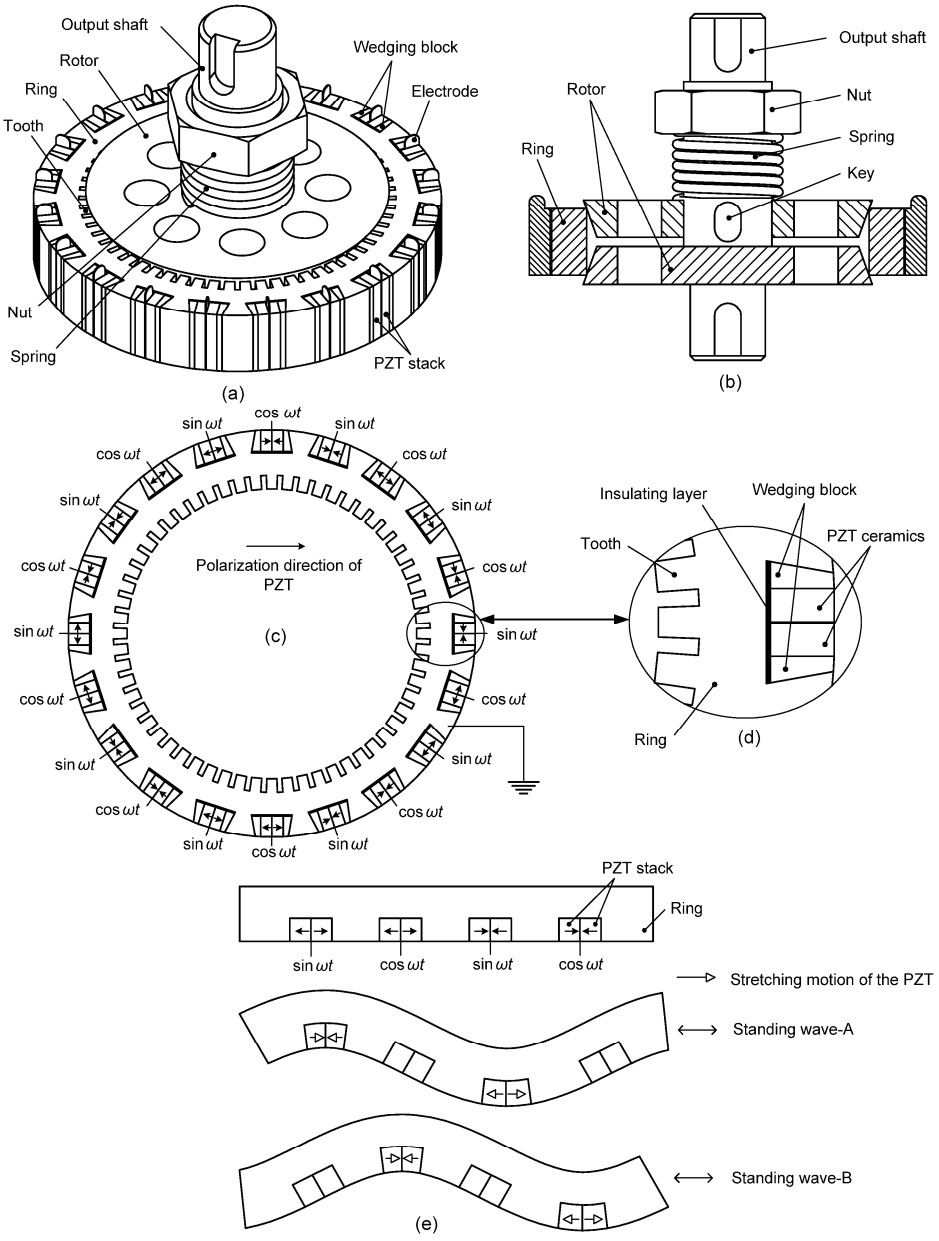

Fig. 1 (a) Structure of the proposed USM, (b) section view, (c) PZT polarization and excitation, (d) partial enlarged drawing, and (e) generations of standing waves

slot by a scale of approximately 5 μm, and this scale is used to provide preloading on the PZT stacks to ensure that they always work under compression stress state. In the embedding of the PZT stacks and the wedging blocks, epoxy adhesive is used at the interfaces to glue them to the stator. To reduce weight, the ring and the rotors are made of aluminum alloy 2A12 in Chinese material standard. The wedging blocks are made of 45# steel in Chinese material standard, and the PZT ceramics material is PZT-41 provided by the Jingdezhen Tonghui Electronics Limited Company, China.

In this study, we intend to produce a bending traveling wave with five wavelengths in the stator, which means that two stand-alone B(0, 5) radial bending mode vibrations with identical frequency and amplitude should be generated in the stator (where 0 and 5 indicate nodal circles and diameters, respectively). Furthermore, these two vibrations should have a quarter wavelength difference on space and a

phase difference of 90° on time. The polarization and excitation manners of the PZT stacks shown in Fig. 1c are established to ensure these necessary conditions for the traveling wave excitation.

In Fig. 1e, one-fifth of the stator, which is one wavelength and contains four PZT stacks, is taken out and developed to be a beam (the teeth and the wedging blocks are ignored for a simple presentation). By applying sine and cosine exciting voltages, stretching vibrations can be generated on the PZT stacks. The stretching vibrations of the first and the third PZT stacks can generate one bending standing wave (standing wave-A), while the other standing wave (standing wave-B) is excited by the second and the fourth PZT stacks. The setting mode of the PZT stacks makes these two flexural standing waves have a quarter wavelength difference on space, while the 90° temporal phase difference is determined by the exciting signals. The degeneration of these two standing waves can result in a flexural traveling wave that rotates round the circumferential direction of the ring. Then, elliptical motions will be formed on the surface particles of the teeth, and the circumferential components of the particle motions can drive the rotors by friction coupling. By changing the phase difference of the exciting signals, the rotary direction of the rotor can be easily altered.

3 Design and analysis of the stator

FEM analysis of the proposed stator was performed to validate the preliminary design (ANSYS 9.0, Ansys Inc., Canonsburg, PA). Firstly, modal analysis was carried out to extract the resonance frequency of B(0, 5) vibration mode of the stator. The voltages applied on the nodes of the PZT in the electrode regions were set to zero. As the thickness of the brass electrode is only 0.1 mm, they were ignored in the stator FEM model. The rubber sheets between the PZT stacks and the bottoms of the slots were also ignored as they had very low rigidity (its thickness is about 0.35 mm). The final dimensions of the duralumin alloy ring are listed in Fig. 2. The thickness of the ring is 15 mm, and the dimensional parameter of the PZT stack is 15 mm×5.1 mm×5 mm. Fig. 3 shows the vibration mode shapes of the proposed stator, where B(0, 5) bending vibration modes can be clearly

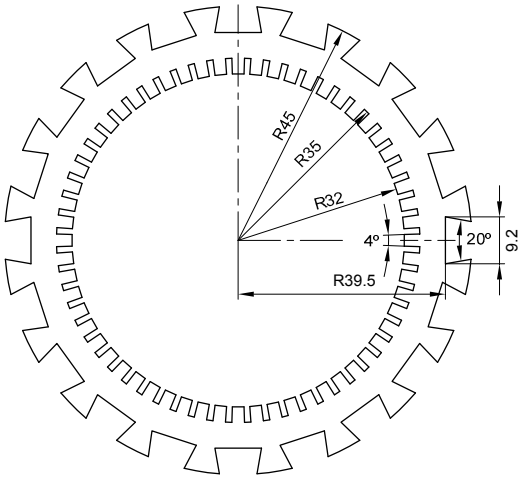

Fig. 2 Dimensions of the duralumin alloy ring (unit: mm)

recognized. There is a quarter wavelength difference on space between the two B(0, 5) modes, which satisfies the condition for composing a traveling wave. Analytical results indicated that the resonance frequencies of the two B(0, 5) modes were equal to be 20.77 kHz.

Then, transient analysis was performed under free edge boundary condition to investigate the excitation of a flexural traveling wave and the particle motions on the driving teeth. Based on the modal analysis results, sine and cosine exciting voltages with effective value of 100 V and frequency of 20.77 kHz were applied to the PZT stacks. By running the transient analysis procedure, the vibration mode shapes shown by Fig. 3 were observed to travel continuously round the stator. To obtain the motion behavior of the driving points, the center nodes on the outer rims of five successive teeth were selected, and Fig. 4 gives the vibration trajectories of the selected nodes in the final period. The gained elliptical trajectories accord with the basic character of traveling wave motor. There is minute diversity among the particle motion trajectories, which indicates that the wave formed in the stator is nearly an ideal traveling wave. Fig. 5 shows the vibration trajectories of five nodes on the center line of one tooth, and the five elliptical trajectories almost overlap each other. The vibration amplitudes in radial and circumferential directions also show that intensive vibration is excited in the proposed stator, which is helpful in improving the output speed and torque.

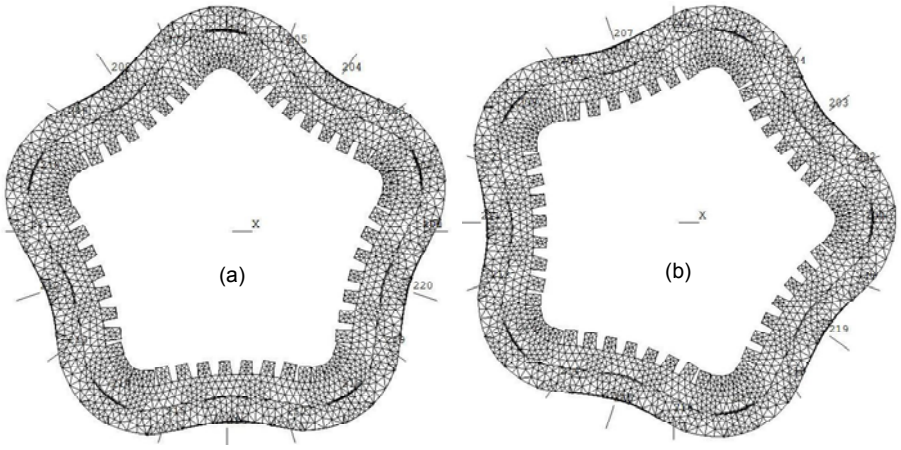

Fig. 3 Two B(0, 5) vibration modes of the stator. (a) Mode-A; (b) Mode-B.

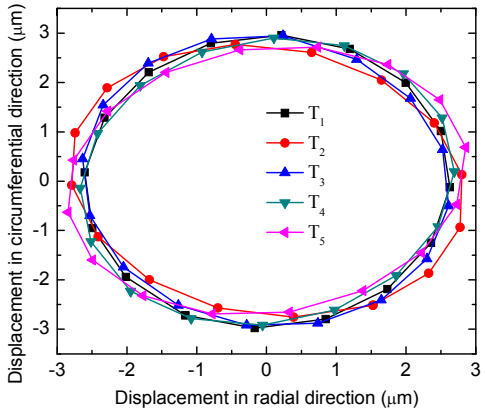

Fig. 4 Vibration trajectories of nodes on five successive teeth T_1–T_5

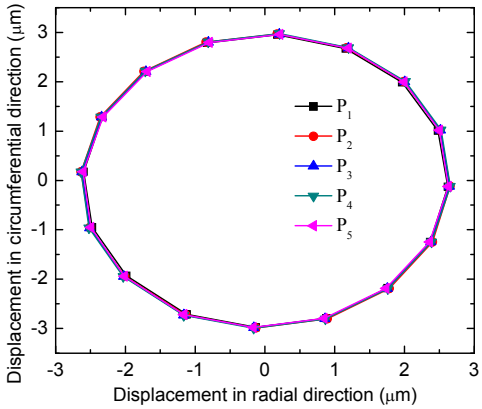

Fig. 5 Vibration trajectories of five nodes P_1–P_5 on one tooth

It is clear that the axial bending mode adopted by the classic ring type traveling wave USM exhibits defects as obvious vibration amplitude diversities of teeth surface particles in both axial and circumferential directions. Thus, the rectifying region between the stator and the rotor should be near to the outer circumference of the stator, which makes it difficult to obtain high output torque and efficiency. Fig. 4 and Fig. 5 state that nearly identical vibrations are generated on the driving particles, which is a significant advantage of the radial bending mode in comparison with the axial one.

Fig. 6 The prototype motor

4 Experiments

A prototype motor was fabricated based on the afore-mentioned FEM analytical results (Fig. 6). The duralumin alloy ring with trapezoid slots and driving teeth was fabricated using a linear cutting machine. The vibration mode shapes and the corresponding resonance frequencies of the prototype were measured

using a scanning laser Doppler vibrometer (PSV-400-M2, Polytec, Germany), and Fig. 7 shows the test results. Considering the vibrometer can only test 1D vibration, part of the outer surface of the stator, about three-quarters wavelength, was selected as the test region during the measurement. Figs. 7a and 7c state that two standing waves are excited under the radial bending mode of the ring type stator, whose phase difference on space is a quarter wavelength. This test result agrees well with the FEM analysis results as shown in Fig. 3. Figs. 7b and 7d indicate that there is no other natural vibration mode in the ambient frequency range of B(0, 5) mode that is obviously excited, which is very favorable for the operational stability of the motor. The resonance frequencies for the two phases are tested to be 19.211 and 19.297 kHz, which are different from the FEM calculated results with discrepancies of 1.559 and 1.473 kHz, respectively. The materials' physical parameters in the FEM model are simply imported from the materials handbook, which may result in these discrepancies. The neglect of the rubber sheets and the electrodes, the machining error and the rigging error are the other reasons that may lead to these discrepancies. There is only 0.086 kHz difference between the two resonance frequencies, which states that the two phases have good consistency.

To evaluate the energy conversion performance of the motor, the elements' parameters in the equivalent circuit model of the stator were measured with the impedance analyzer (4294A, Agilent Inc., USA), (Table 1). Thus, the concerned parameters can be calculated, and the quality factor Q_m may be obtained:

$$Q_m = \frac{1}{R_m}\sqrt{\frac{L_m}{C_m}}, \tag{1}$$

where R_m, L_m and C_m are the dynamic resistance, inductance and capacitance in the mechanical branch of the equivalent circuit, respectively. Another important parameter is the electromechanical dynamic coupling factor k, which may be calculated by

Table 1 Measured equivalent circuit parameters and calculated Q_m and k

Phase	R_m (Ω)	L_m (mH)	C_m (pF)
A	992.385	460.777	146.680
B	1020.98	439.702	153.978
Phase	C_a (nF)	Q_m	k (%)
A	7.02833	56.48	14.30
B	6.93361	56.32	14.74

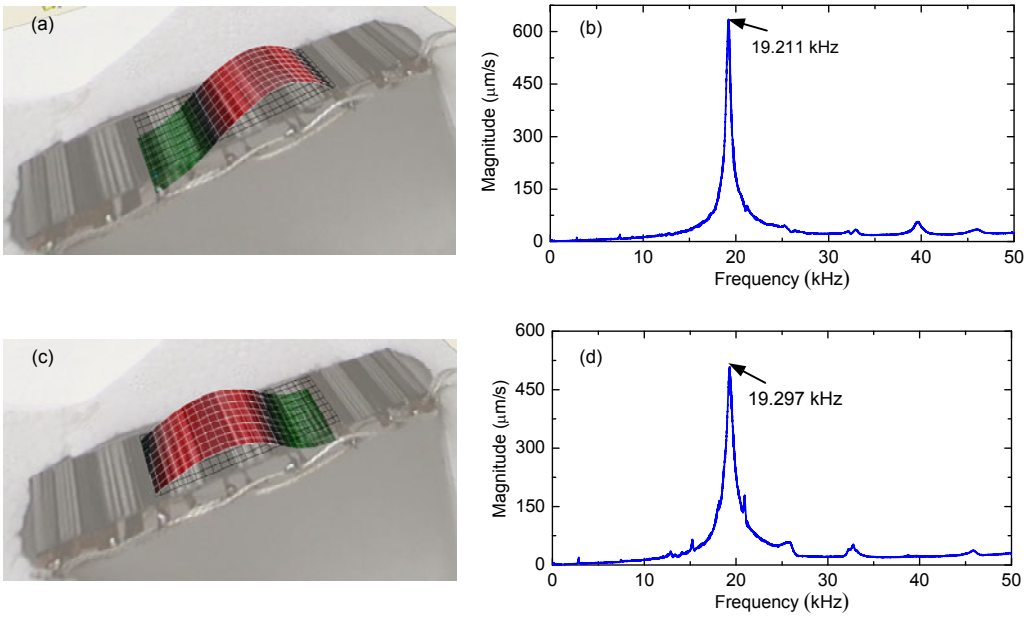

Fig. 7 Vibration test results of the prototype

(a) Vibration shape of phase-A; (b) Vibration velocity response spectrum under phase-A excitation; (c) Vibration shape of phase-B; (d) Vibration velocity response spectrum under phase-B excitation

$$k=\sqrt{\frac{C_{\mathrm{m}}}{C_{\mathrm{a}}+C_{\mathrm{m}}}}, \tag{2}$$

where C_{a} stands for the clamped capacitance.

Finally, two phases of exciting voltages that have a phase difference of 90° on time are applied on the PZT elements to test the mechanical output ability of the prototype. Fig. 8 gives the output speed under different exciting frequencies on a no-load condition (effective value of input voltage 150 V). The motor achieves a maximal speed of 126 r/min as the exciting frequency is approximately 19.20 kHz. Then, the frequency and effective value of input voltages are fixed to be 19.20 kHz and 150 V, respectively, and Fig. 9 gives the output speed and power under different torques.

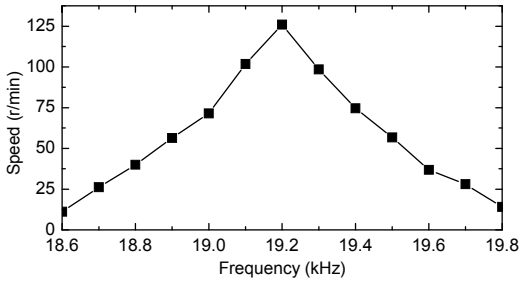

Fig. 8 Motor speed under different exciting frequencies

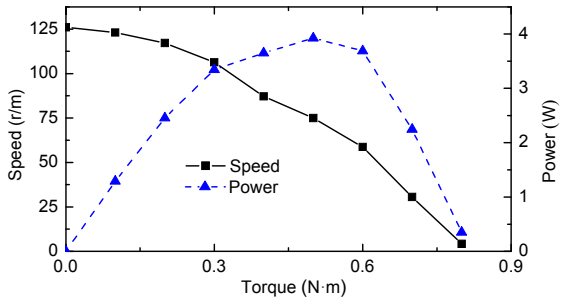

Fig. 9 Motor speed and power under different torques

Fig. 9 shows that a maximal torque of 0.8 N·m is achieved by the prototype, while the maximal power is about 3.9 W. As the rotors are driven by the frictional forces between the interfaces, the output torque can be improved by increasing the preload. Note that no frictional material was used in the prototype, and the adopting of appropriate frictional materials for the interface will significantly enhance the output features of the motor. Furthermore, two conical rotors were used in the prototype, and the end rims of teeth served as the driving tips. This match has not fully used the same elliptical vibration on the driving particles. Thus, the elastic rotor that has cylindrical contact with the inner surfaces of the teeth will obviously improve the output torque.

5 Conclusions

A new traveling wave USM using a thick ring stator with nested PZT stacks is proposed. This new design not only inherits the advantages of both the classic ring type traveling wave USM and the motor excited by sandwich transducer, but also overcomes their disadvantages. The high electromechanical coupling factor d_{33} operating mode of the PZT favors the motor has the potential to obtain powerful mechanical output. The nesting structure of the PZT stacks ensures that no tensile failure will occur under intensive vibration. There is no matching problem between different type vibration modes in this design, which makes the design procedure quite flexible. The elliptical trajectories of driving particles show a significant advantage of the proposed motor in obtaining nearly identical vibrations on the driving teeth. After the fabrication of a prototype motor, the maximal torque and power of 0.8 N·m and 3.9 W are achieved, and they are relatively high values for traveling wave USM when considering that the weight of the stator is only 0.18 kg.

Future study will focus on the following aspects: optimizing the structure of the motor to improve the electromechanical coupling factor, tuning the resonance frequency larger than 20 kHz by decreasing the radial dimensions of the stator, testing different frictional materials and applying larger preload to the interface, and designing an elastic rotor that has cylindrical contact with the inner surfaces of the teeth.

References

Asumi, K., Fukunaga, R., Fujimura, T., Kurosawa, M.K., 2009. Miniaturization of a V-shape transducer ultrasonic motor. *Japanese Journal of Applied Physics*, **48**:07GM02. [doi:10.1143/JJAP.48.07GM02]

Chen, W.S., Liu, Y.X., Liu, J.K., Shi, S.J., 2010. A linear ultrasonic motor using bending vibration transducer with double driving feet. *Ferroelectronics*, **400**:221-230. [doi:10.1080/00150193.2010.505544]

Iula, A., Corbo, A., Pappalardo, M., 2010. FE analysis and experimental evaluation of the performance of a

travelling wave rotary motor driven by high power ultrasonic transducers. *Sensors and Actuators A: Physical*, **160**:94-100. [doi:10.1016/j.sna.2010.03.037]

Jin, J.M., Zhao, C.S., 2008. A novel traveling wave ultrasonic motor using a bar shaped transducer. *Journal of Wuhan University of Technology: Materials Science Edition*, **23**(6):961-963. [doi:10.1007/s11595-008-6961-1]

Li, X., Chen, W.S., Xie, T., Liu, J.K., 2007. Novel high torque bearingless two-sided rotary ultrasonic motor. *Journal of Zhejiang University-SCIENCE A*, **8**(5):786-792. [doi:10.1631/jzus.2007.A0786]

Liu, Y.X., Chen, W.S., Liu, J.K., Shi, S.J., 2010a. A high-power linear ultrasonic motor using longitudinal vibration transducers with single foot. *IEEE Transactions on Ultrasonics, Ferroelectrics Frequency Control*, **57**:1860-1867. [doi:10.1109/TUFFC.2010.1625]

Liu, Y.X., Chen, W.S., Liu, J.K., Shi, S.J., 2010b. A cylindrical traveling wave ultrasonic motor using longitudinal vibration transducers. *Ferroelectronics*, **409**:117-127. [doi:10.1080/00150193.2010.485968]

Liu, Y.X., Chen, W.S., Liu, J.K., Shi, S.J., 2010c. A cylindrical traveling wave ultrasonic motor using longitudinal and bending composite transducer. *Sensors and Actuators A: Physical*, **161**:158-163. [doi:10.1016/j.sna.2010.06.001]

Luo, L.H., Zhu, H., Zhao, C.S., Wang, F.F., Luo, H.S., 2008. A cylinder-shaped miniature ultrasonic motor based on $Pb(Mg_{1/3}Nb_{2/3})O_3$-$PbTiO_3$ single crystals. *Journal of Intelligent Material Systems and Structures*, **19**:1457-1461. [doi:10.1177/1045389X07088062]

Oh, J.H., Jung, H.E., Lee, J.S., Lim, K.J., Kim, H.H., Ryu, B.H., Park, D.H., 2009. Design and performance of high torque ultrasonic motor for application of automobile. *Journal of Electroceramics*, **22**:150-155. [doi:10.1007/s10832-008-9434-1]

Park, J.S., Kim, S.T., Kim, J.W., 2005. Ultrasonic linear motor using L1-B4 mode and its analysis. *Japanese Journal of Applied Physics*, **44**(1A):412-416. [doi:10.1143/JJAP.44.412]

Petit, L., Gonnard, P., 2009. A multilayer TWILA ultrasonic motor. *Sensors and Actuators A: Physical*, **149**(1):113-119. [doi:10.1016/j.sna.2008.09.020]

Shi, Y.L., Zhao, C.S., Huang, W.Q., 2010. Linear ultrasonic motor with wheel-shaped stator. *Sensors and Actuators A: Physical*, **161**:205-209. [doi:10.1016/j.sna.2010.05.009]

Sun, D.M., Wang, S., Sakurai, J., Choi, K.B., Shimokohbe, A., Hata, S., 2010. A piezoelectric linear ultrasonic motor with the structure of a circular cylindrical stator and slider. *Smart Materials and Structures*, **19**:045008. [doi:10.1088/0964-1726/19/4/045008]

Ting, Y., Chen, L.C., Li, C.C., Huang, J.L., 2007. Traveling-wave piezoelectric linear motor part I: The stator design. *IEEE Transactions on Ultrasonics, Ferroelectrics Frequency Control*, **54**(4):847-853. [doi:10.1109/TUFFC.2007.319]

Ueha, S., Tomikawa, Y., 1993. Ultrasonic Motors: Theory and Applications. Clarendon Press, Oxford.

Zhang, X.L., Tan, Y.H., 2008. Modeling of ultrasonic motor with dead-zone based on Hammerstein model structure. *Journal of Zhejiang University-SCIENCE A*, **9**(1):58-64. [doi:10.1631/jzus.A071146]

Zhao, C.S., 2010. Ultrasonic Motors Technologies and Applications. Science Press, Beijing.

2010 JCR of Thomson Reuters for *JZUS-A* and *JZUS-B*

ISI Web of Knowledge℠

Journal Citation Reports®

WELCOME HELP RETURN TO LIST

2010 JCR Science Edition

Journal: Journal of Zhejiang University-SCIENCE A

Mark	Journal Title	ISSN	Total Cites	Impact Factor	5-Year Impact Factor	Immediacy Index	Citable Items	Cited Half-life	Citing Half-life
☐	J ZHEJIANG UNIV-SC A	1673-565X	442	0.322		0.050	120	3.7	7.1

Journal: Journal of Zhejiang University-SCIENCE B

Mark	Journal Title	ISSN	Total Cites	Impact Factor	5-Year Impact Factor	Immediacy Index	Citable Items	Cited Half-life	Citing Half-life
☐	J ZHEJIANG UNIV-SC B	1673-1581	770	1.027		0.137	124	3.5	7.5